Electronic version of an article published as Journal of Computational Acoustics , Volume 19, Issue 2, 2011, Pages: 139-154, DOI: 10.1142/S0218396X11004419

A 3D MODEL TO SIMULATE VIBRATIONS IN A LAYERED MEDIUM WITH STOCHASTIC MATERIAL PARAMETERS

W. KREUZER, H. WAUBKE, G. RIECKH and P. BALAZS

Austrian Academy of Sciences, Acoustics Research Institute, Wohllebengasse 12-14, 1040 Vienna, Austria
wolfgang.kreuzer@oeaw.ac.at

Received (Day Month Year)
Revised (Day Month Year)

A major problem for the simulation of the propagation of vibrations in ground layers is the fact that it is almost impossible to determine the material parameters needed for a numerical model exactly. In this work, we present a 3D-model for layered soil, where in each layer the shear modulus is modeled as a stochastic process. Using the Karhunen Loeve expansion, the polynomial chaos expansion, and the Fourier transform, the stochastic system can be transformed into a linear system of equations in the wavenumber frequency domain. Unfortunately, the size of this system becomes very large and - contrary to a deterministic system - the stochastic system can no longer be decoupled for every wavenumber in the spatial Fourier domain. To solve this system efficiently, we propose an iteration procedure where the system is split into a deterministic and a stochastic part. As an external load on top of the ground, we use a vibrating box load moving along the x-axis. We discuss implementational details and present simulation results.

Keywords: Stochastic finite elements, soil model, moving loads

1. Introduction

There is a wide range of numerical models to predict the propagation of vibrations in ground layers (see for example [1,2,3,4]). The major problem for soil models is the fact that material parameters for the medium are not known exactly. Often these parameters are determined based on small measured samples, which are not able to give an exact impression of the soil[5]. If only small variations of the material parameters are allowed, models based on perturbation theory can be used. But such models neglect a randomness in the solution caused by a large randomness in the material parameters [5,6]. Alternative approaches are models based on the Monte Carlo method, or models based on stochastic finite elements[6], which will be the basis for our method (see also Xiu[7] for a review of numerical methods for stochastic computations).

In this paper, we introduce an approach that is based on the idea of stochastic finite elements[6]. One of the material parameters (the shear modulus) is modeled as a stochastic process[a]. It is assumed that the shear modulus G has a mean value $G_0(z)$, which only depends on the depth z. Additionally, the covariance of G is given by a bounded function $C(\mathbf{x}_1, \mathbf{x}_2)$, which is scaled by a constant factor G_s. This factor is introduced to simplify notation and implementation. G is expanded into a series of orthogonal random variables

[a]We only assume the shear modulus G to be stochastic; the idea can easily be expanded to the mass density.

$\xi_\ell(\theta)$ and deterministic functions $f_\ell(x, y)$ using the Karhunen Loeve expansion (KLE). The unknown displacements, which are also stochastic, are expanded using the polynomial chaos expansion (PCE).

Starting from a variational formulation of the problem, a linear system of equations is derived by dividing the soil into thin layers and by making a finite-element-like ansatz with respect to the depth z for the unknown displacements in the x, y and z directions. After a variation in each of these layers, the unknown functions are expanded using the PCE, and the system is projected onto the space spanned by finitely many chaos polynomials. A Fourier transform with respect to the horizontal spatial coordinates and time is made, and a linear system can be derived for given grid points in the transformed domain. On top of the soil, a vibrating load that moves along the x-axis with a velocity v is applied.

As the size of the linear system is too big to be solved directly, an iteration is used. The system is split into a deterministic part, which has a sparse block diagonal system matrix $\mathbf{K_d}$, and a stochastic part represented by a dens matrix $\mathbf{K_s}$. A LU-decomposition of $\mathbf{K_d}$ can be done efficiently because of its sparse structure. Thus the solution is calculated using an iteration: $\mathbf{K_d}\hat{\mathbf{x}}_n = \hat{\mathbf{b}}_{\text{Ext}} - \mathbf{K_s}\hat{\mathbf{x}}_{n-1}$ with $\mathbf{K_d}\hat{\mathbf{x}}_0 = \hat{\mathbf{b}}_{\text{Ext}}$.

This paper is an extension of a former paper[8] to 3D. Additionally, we discuss the use of a moving load as an excitation force on top of the soil and look more detailed on the generation of the linear system. We only give a brief introduction of the main stochastic tools, and concentrate more on practical issues, the implementation of a moving load and the linear system of equations. The paper is organized as follows: The main differential equation is described in Section 2. In Section 3, a short overview of the two stochastic expansions KLE and PCE are given. As these two expansions have a direct influence on the size of the linear system of equations, we introduce an iteration procedure to solve the system efficiently, which is described in Section 4. Finally, we discuss some implementational issues in Section 5, and also present results for an example.

2. Problem formulation

The governing equation can be derived by setting the variance of the total energy of the system to zero, i.e.

$$\delta\left(\sum_{n=1}^{N}\Pi_n\right) = 0, \tag{1}$$

where Π_n is the total energy in one single layer starting at depth z_n, with width d and density ρ. If we denote the vector of the displacements in the x, y and z directions by $\tilde{\mathbf{u}} = (u, v, w)$, and the vector containing the stresses and strains as $\boldsymbol{\sigma}$ and $\boldsymbol{\varepsilon}$, Π_n can be formulated as:

$$\Pi_n = \int_{x,y,t=-\infty}^{\infty} \left(\int_{z=z_n}^{z_n+d} \boldsymbol{\sigma}^{\boldsymbol{T}} \boldsymbol{\varepsilon} + \rho \left(\frac{\partial}{\partial t} \tilde{\mathbf{u}} \right)^2 dz \right) + f_{\mathrm{Ext}} w|_{z=0} dt\, dy\, dx =$$

$$= \int_{t,x,y} \int_{z} \frac{2(1-\nu)}{1-2\nu} G(\theta) \left(\left(\frac{\partial u}{\partial x} \right)^2 + \left(\frac{\partial v}{\partial y} \right)^2 + \left(\frac{\partial w}{\partial z} \right)^2 \right) +$$

$$+ \frac{4\nu}{1-2\nu} G(\theta) \left(\frac{\partial u}{\partial x}\frac{\partial v}{\partial y} + \frac{\partial v}{\partial y}\frac{\partial w}{\partial z} + \frac{\partial u}{\partial x}\frac{\partial w}{\partial z} \right) +$$

$$+ G(\theta) \left(\left(\frac{\partial u}{\partial y} + \frac{\partial v}{\partial x} \right)^2 + \left(\frac{\partial v}{\partial z} + \frac{\partial w}{\partial y} \right)^2 + \left(\frac{\partial w}{\partial x} + \frac{\partial u}{\partial z} \right)^2 \right) -$$

$$- \rho \left(\left(\frac{\partial u}{\partial t} \right)^2 + \left(\frac{\partial v}{\partial t} \right)^2 + \left(\frac{\partial w}{\partial t} \right)^2 \right) dz - 2 f_{\mathrm{Ext}} w_{|z=0} dt dy dx. \tag{2}$$

The material is assumed to be isotropic, the shear modulus $G(\theta)$ is dependent on the stochastic variable θ. The Poisson ratio ν and the density ρ are deterministic variables. On top of the layered soil (at $z = 0$), we assume an external force f_{Ext} pointing downwards.

Under the last layer, a (non stochastic) half space with appropriate boundary conditions ($\tilde{\mathbf{u}} \to \mathbf{0}$ as $z \to \infty$) is added to prevent unwanted reflections in the z-direction as $z \to \infty$. The half space is assumed to have deterministic material parameters. Thus the displacements can be formulated with the help of the following potentials[9]:

$$\Phi = A_1 e^{\lambda_1 z} + A_2 e^{-\lambda_1 z} \tag{3}$$

$$\Psi^{[1]} = B_1 e^{\lambda_2 z} + B_2 e^{-\lambda_2 z} \tag{4}$$

$$\Psi^{[2]} = C_1 e^{\lambda_2 z} + C_2 e^{-\lambda_2 z} \tag{5}$$

with

$$\lambda_1 = -\mathrm{i}\sqrt{\frac{\omega^2}{c_1^2} - k_x^2 - k_y^2}, \;\; c_1 = \sqrt{\tfrac{\lambda+2\mu}{\rho}}$$

$$\lambda_2 = -\mathrm{i}\sqrt{\frac{\omega^2}{c_2^2} - k_x^2 - k_y^2}, \quad c_2 = \sqrt{\tfrac{\mu}{\rho}}\,,$$

where $\mathrm{i}^2 = -1$, and λ, μ and ρ are the material parameters. The unknown A_1, A_2, B_1, B_2, C_1 and C_2 are determined by the boundary conditions for the half space layer. The radiation condition implies that the exponential terms with positive exponent (i.e. those for which the exponential function does not decline for $z \to \infty$) should not contribute to the solution, or in other words the far field components have to be zero. This is achieved by setting the appropriate coefficients in Eqs. (3) to (5) to zero.

The coupling of the half space to the layered soil is achieved through continuity conditions at the layer boundary. Please note that even though the shear modulus G of the

half space does not depend on the stochastic parameter, the displacements still have to be expanded using the PCE.

To transform Eq. (2) into a linear system of equations, we divide the soil into thin layers, and the unknown displacements u, v and w are approximated with a polynomial basis $\boldsymbol{\phi} = (\phi_0(z), \ldots, \phi_M(z))^T$ (in our example we use 2nd order B-splines)

$$\begin{aligned} u(x,y,z,t,\theta) &\approx \sum_{i=0}^{M} \mathbf{u}_i(x,y,t,\theta)\phi_i(z) = \boldsymbol{\phi}^T\mathbf{u}, \\ v(x,y,z,t,\theta) &\approx \sum_{i=0}^{M} \mathbf{v}_i(x,y,t,\theta)\phi_i(z) = \boldsymbol{\phi}^T\mathbf{v}, \\ w(x,y,z,t,\theta) &\approx \sum_{i=0}^{M} \mathbf{w}_i(x,y,t,\theta)\phi_i(z) = \boldsymbol{\phi}^T\mathbf{w}. \end{aligned} \tag{6}$$

Variation with respect to the unknowns u_i, v_i and w_i in Eq. (6) transforms Eq. (2) into a system of 3 times $(M+1)$ equations which is dependent on the horizontal coordinates x and y, the time t, and the stochastic parameter θ. In compact notation, this system can be written as

$$\begin{aligned} &\frac{\partial}{\partial x}\left(\frac{2(1-\nu)}{1-2\nu}G(\theta)\boldsymbol{\Phi}\frac{\partial \mathbf{u}}{\partial x} + \frac{2\nu G(\theta)}{1-2\nu}\left(\boldsymbol{\Phi}\frac{\partial \mathbf{v}}{\partial y} + \boldsymbol{\Phi}'^T\mathbf{w}\right)\right) + \\ &\quad + \boldsymbol{\Phi}\frac{\partial}{\partial y}\left(G(\theta)\left(\frac{\partial \mathbf{u}}{\partial y} + \frac{\partial \mathbf{v}}{\partial x}\right)\right) + G(\theta)\left(\bar{\boldsymbol{\Phi}}\mathbf{u} + \boldsymbol{\Phi}'\frac{\partial \mathbf{w}}{\partial x}\right) - \rho\boldsymbol{\Phi}\frac{\partial^2}{\partial t^2}\mathbf{u} = \mathbf{0} \\ &\frac{\partial}{\partial y}\left(\frac{2(1-\nu)}{1-2\nu}G(\theta)\boldsymbol{\Phi}\frac{\partial \mathbf{v}}{\partial y} + \frac{2\nu G(\theta)}{1-2\nu}\left(\boldsymbol{\Phi}\frac{\partial \mathbf{u}}{\partial x} + \boldsymbol{\Phi}'^T\mathbf{w}\right)\right) + \\ &\quad + \boldsymbol{\Phi}\frac{\partial}{\partial x}\left(G(\theta)\left(\frac{\partial \mathbf{u}}{\partial y} + \frac{\partial \mathbf{v}}{\partial x}\right)\right) + G(\theta)\left(\bar{\boldsymbol{\Phi}}\mathbf{v} + \boldsymbol{\Phi}'\frac{\partial \mathbf{w}}{\partial y}\right) - \rho\boldsymbol{\Phi}\frac{\partial^2}{\partial t^2}\mathbf{v} = \mathbf{0} \\ &\frac{\partial}{\partial x}\left(G(\theta)\boldsymbol{\Phi}'^T\mathbf{u} + G(\theta)\boldsymbol{\Phi}\frac{\partial \mathbf{w}}{\partial x}\right) + \frac{\partial}{\partial y}\left(G(\theta)\boldsymbol{\Phi}'^T\mathbf{v} + G(\theta)\boldsymbol{\Phi}\frac{\partial \mathbf{w}}{\partial y}\right) - \\ &\quad \frac{2\nu G(\theta)}{1-2\nu}\left(\boldsymbol{\Phi}'\frac{\partial \mathbf{u}}{\partial x} + \boldsymbol{\Phi}'\frac{\partial \mathbf{v}}{\partial y}\right) + \frac{2(1-\nu)}{1-2\nu}G(\theta)\bar{\boldsymbol{\Phi}}\mathbf{w} - \rho\boldsymbol{\Phi}\frac{\partial^2}{\partial t^2}\mathbf{w} = f_{\mathrm{Ext}}\boldsymbol{\phi}(0), \end{aligned} \tag{7}$$

where the entries[b] of the matrices $\boldsymbol{\Phi}, \boldsymbol{\Phi}'$ and $\bar{\boldsymbol{\Phi}}$ are defined by $[\boldsymbol{\Phi}]_{ij} = \int_{z=z_n}^{z_n+d} \phi_i(z)\phi_j(z)dz$, $[\boldsymbol{\Phi}']_{ij} = \int_{z=z_n}^{z_n+d} \phi_i(z)\frac{d\phi_j}{dz}(z)dz$ and $[\bar{\boldsymbol{\Phi}}]_{ij} = \int_{z=z_n}^{z_n+d} \frac{d\phi_i}{dz}(z)\frac{d\phi_j}{dz}(z)dz$. $\boldsymbol{\phi}$ is the vector of the shape functions $\phi_j(z)$, $\mathbf{u} = (u_0, \ldots, u_M)^T, \mathbf{v} = (v_0, \ldots, v_M)^T$, and $\mathbf{w} = (w_0, \ldots, w_M)^T$. With the subdivision into different horizontal layers it is also possible to use material parameters that are dependent on the depth z.

[b] $[\mathbf{A}]_{ij}$ denotes the entry in the i-th row and the j-th column of a matrix $\mathbf{A}$.

3. Stochastic Expansions

3.1. *Karhunen Loeve Expansion (KLE)*

With the KLE[6,10,11,12], it is possible to expand a random process with a known covariance function into a linear combination of normalized uncorrelated random variables $\xi_\ell(\theta)$ and deterministic functions dependent on the horizontal coordinates. It is also known that the n-term KLE approximation has minimizing error properties[6]. The stochastic shear modulus G is assumed to be complex valued, which allows modeling of damping effects. It has a mean value $G_0(z)$, which is only dependent on the depth z, and a bounded covariance function. The covariance function is assumed to be given by a real valued function $C(\mathbf{x}_1, \mathbf{x}_2)$ multiplied with a constant scaling factor G_s, which can be complex. Using these assumptions, the KLE can be applied to $C(\mathbf{x}_1, \mathbf{x}_2)$, and G can be expanded into:

$$G(x, y, z, \theta) = G_0(z) + G_s \sum_{\ell=0}^{\infty} \sqrt{\lambda_\ell} f_\ell(x, y) \xi_\ell(\theta). \tag{8}$$

λ_ℓ and f_ℓ are the eigenvalues and (orthonormal) eigenfunctions of $C(\mathbf{x_1}, \mathbf{x_2})$, $\mathbf{x_1}, \mathbf{x_2} \in \mathbb{R}^2$, and are given by the solution of the Fredholm equation

$$\int_{\mathbb{R}^2} C(\mathbf{x_1}, \mathbf{x_2}) f_\ell(\mathbf{x_2}) d\mathbf{x_2} = \lambda_\ell f_\ell(\mathbf{x_1}). \tag{9}$$

Moreover, if the random process is Gaussian, $\xi_\ell(\theta)$ are independent Gaussian distributed random variables.

There are several methods to solve Eq. (9). For some distributions, an analytical solution can be found, but in most cases, the eigenpairs have to be calculated numerically[6,11,13].

3.2. *Polynomial Chaos Expansion*

For the unknown displacements, the polynomial chaos expansion (PCE)[6,14,15,16] is used. It was originally defined by Wiener[17], and allows an expansion of square integrable random functions into a series of Hermite polynomials Γ_j, which form an orthogonal set with respect to Gaussian normal distribution, i.e. $\langle \Gamma_i, \Gamma_j \rangle = \mathbb{E}(\Gamma_i \Gamma_j) = \int_{-\infty}^{\infty} \Gamma_i \Gamma_j e^{-\xi^2/2} d\xi = 0$ for $i \neq j$ [6]. It can be shown that the PCE converges for arbitrary random functions with finite second-order moments; however an optimal exponential convergence rate can only be expected for Gaussian random functions[16]. Later, the theory of PCE was expanded to also guarantee exponential convergence rates also for certain non-Gaussian distributions (generalized PCE, Askey PCE)[15,16].

Using the PCE, the unknown displacements can be further expanded into

$$u(x,y,z,t,\theta) \approx \sum_{i=0}^{M}\sum_{j=0}^{N} u_{ij}(x,y,t)\phi_i(z)\Gamma_j(\boldsymbol{\xi}) = \boldsymbol{\phi}^T\mathbf{U}\boldsymbol{\Gamma},$$
$$v(x,y,z,t,\theta) \approx \sum_{i=0}^{M}\sum_{j=0}^{N} v_{ij}(x,y,t))\phi_i(z)\Gamma_j(\boldsymbol{\xi}) = \boldsymbol{\phi}^T\mathbf{V}\boldsymbol{\Gamma},$$
$$w(x,y,z,t,\theta) \approx \sum_{i=0}^{M}\sum_{j=0}^{N} w_{ij}(x,y,t)\phi_i(z)\Gamma_j(\boldsymbol{\xi}) = \boldsymbol{\phi}^T\mathbf{W}\boldsymbol{\Gamma}, \tag{10}$$

where $\boldsymbol{\xi}$ is the vector of random variables ξ_ℓ from the KLE. The length N of the PCE is dependent on the maximum order of chaos polynomials and the expansion length of the KLE.

In general, there are two possible ways to calculate the unknown coefficients u_{ij}, v_{ij} and w_{ij} in Eq. (10). Berveille et. al[18] describe a non intrusive approach, which uses a combination of sampling and least square solutions to determine the unknown coefficients. In our model, a direct (intrusive) approach using projections of the system onto the space spanned by the Γ_j (see also Ghanem and Spanos[6]) is used. This approach has the advantage that no sampling is necessary, but, on the other hand, the size of the system matrix gets larger.

4. The Linear System of Equations

To transform Eq. (7) into a linear system of equations, the KLE is applied to the shear modulus, and the unknown displacements are expanded using the PCE (see Eq. (10)). The system is then projected onto the space spanned by all chaos polynomials. With the Fourier transform with respect to the spatial coordinates x and y and the time t, all derivative operators are transformed into simple multiplication operators. As a final step, the (k_x, k_y)-domain is discretized with an equidistant collocation grid $(\mathbf{k_x}, \mathbf{k_y})$.

With the KLE (Eq. (8)), it is possible to split the shear modulus into a deterministic part containing only the mean value G_0 and a stochastic part containing the rest. In the same way, it is possible to split the whole system into a deterministic and a stochastic part

$$G_0\mathbf{A}_d^{[1]}(\hat{\mathbf{U}},\hat{\mathbf{V}},\hat{\mathbf{W}}) + G_s\sum_\ell\left(\mathbf{A}_\ell^{[1]}(\hat{\mathbf{U}})+\mathbf{A}_\ell^{[2]}(\hat{\mathbf{V}})+\mathbf{A}_\ell^{[3]}(\hat{\mathbf{W}})\right) - \rho\omega^2\boldsymbol{\Phi}\hat{\mathbf{U}}\mathbf{D}_\Gamma = \mathbf{0}$$
$$G_0\mathbf{A}_d^{[2]}(\hat{\mathbf{U}},\hat{\mathbf{V}},\hat{\mathbf{W}}) + G_s\sum_\ell\left(\mathbf{A}_\ell^{[4]}(\hat{\mathbf{U}})+\mathbf{A}_\ell^{[5]}(\hat{\mathbf{V}})+\mathbf{A}_\ell^{[6]}(\hat{\mathbf{W}})\right) - \rho\omega^2\boldsymbol{\Phi}\hat{\mathbf{V}}\mathbf{D}_\Gamma = \mathbf{0}$$
$$G_0\mathbf{A}_d^{[3]}(\hat{\mathbf{U}},\hat{\mathbf{V}},\hat{\mathbf{W}}) + G_s\sum_\ell\left(\mathbf{A}_\ell^{[7]}(\hat{\mathbf{U}})+\mathbf{A}_\ell^{[8]}(\hat{\mathbf{V}})+\mathbf{A}_\ell^{[9]}(\hat{\mathbf{W}})\right) - \rho\omega^2\boldsymbol{\Phi}\hat{\mathbf{W}}\mathbf{D}_\Gamma = \hat{\mathbf{F}}_{\mathrm{Ext}}, \tag{11}$$

where $\hat{\mathbf{U}}, \hat{\mathbf{V}}$ and $\hat{\mathbf{W}}$ contain the Fourier coefficients of $\mathbf{U}, \mathbf{V}$ and $\mathbf{W}$. $\mathbf{D}_\Gamma = \mathrm{diag}(\mathbb{E}(\Gamma_0^2), \ldots, \mathbb{E}(\Gamma_N^2))$ is a diagonal matrix containing the expectation of Γ_i^2. The entries of $\hat{\mathbf{F}}_{\mathrm{ext}}$ are given by $[\hat{\mathbf{F}}_{\mathrm{Ext}}]_{ij} = \hat{f}_{\mathrm{Ext}}(k_x, k_y) \cdot \phi_i(0) \cdot \mathbb{E}(\Gamma_j)$, where f_{Ext} is the external load

function. For a detailed description of $\mathbf{A}_d^{[i]}$ and $\mathbf{A}_\ell^{[i]}$, please refer to Appendix A. Because of the orthogonality of the chaos polynomials, and the fact that $\Gamma_0 \equiv c$ (a polynomial of degree 0), we get $\mathbb{E}(\Gamma_j) = \mathbb{E}(1 \cdot \Gamma_j) = \frac{1}{c}\langle \Gamma_0, \Gamma_j \rangle = 0$ for $j > 0$, and $\hat{\mathbf{F}}_{\text{Ext}}$ is thus sparse and can be reduced to a vector.

As traffic induced noise and vibrations are a major problem, a lot of different models for moving loads exist[19,20,21,22]. In our approach, the load can either be modeled with a point load, or with a boxed load moving with velocity v along the x axis. It is assumed that the load oscillates with a frequency ω_0.

A point load with strength P is given by

$$f_{\text{Ext}}(x, y, t) = P\delta(x - vt)\delta(y)\cos(2\pi\omega_0 t), \tag{12}$$

the box load with length b_1 and width b_2 is modeled by

$$f_{\text{Ext}}(x, y, t) = \frac{P}{b_1 b_2}\Pi\left(\frac{x - vt}{b_1}\right)\Pi\left(\frac{y}{b_2}\right)\cos(2\pi\omega_0 t), \tag{13}$$

where $\delta(x)$ denotes the Dirac delta functional, and the function Π is defined as

$$\Pi(x) = \begin{cases} 0 & |x| > \frac{1}{2} \\ \frac{1}{2} & |x| = \frac{1}{2} \\ 1 & |x| < \frac{1}{2} \end{cases}.$$

The "stochastic part" of the system contains the eigenfunctions $f_\ell(x, y)$ and the variables $\xi(\theta)$ (see Eq. (8)), which couples the system for all wavenumbers and all chaos polynomials. For example $\mathbf{A}_\ell^{[1]}$ is given by:

$$\begin{aligned}\left[\mathbf{A}_\ell^{[1]}(\hat{\mathbf{U}}(k_x, k_y))\right]_{ij} = \\ \frac{2(1-\nu)}{1-2\nu}\int_{-\infty}^{\infty}\int_{-\infty}^{\infty} k_x k_x' \hat{f}_\ell(k_x - k_x', k_y - k_y')\left[\mathbf{\Phi}\hat{\mathbf{U}}(k_x', k_y')\mathbf{\Gamma}_\ell\right]_{ij} dk_x' dk_y' + \\ + \int_{-\infty}^{\infty}\int_{-\infty}^{\infty} k_y k_y' \hat{f}_\ell(k_x - k_x', k_y - k_y')\left[\mathbf{\Phi}\hat{\mathbf{U}}(k_x', k_y')\mathbf{\Gamma}_\ell\right]_{ij} dk_x' dk_y' - \\ - \int_{-\infty}^{\infty}\int_{-\infty}^{\infty} \hat{f}_\ell(k_x - k_x', k_y - k_y')\left[\bar{\mathbf{\Phi}}\hat{\mathbf{U}}(k_x', k_y')\mathbf{\Gamma}_\ell\right]_{ij} dk_x' dk_y'.\end{aligned} \tag{14}$$

$\hat{f}_\ell(k_x, k_y)$ are the Fourier transforms of the KLE-eigenfunctions $f_\ell(x, y)$, $[\mathbf{\Gamma}_\ell]_{ij}$ is given by the expectation of the product $\xi_\ell \cdot \Gamma_i \cdot \Gamma_j$, where ξ_ℓ and Γ_i are defined in Eqs. (8) and (10).

The deterministic part, on the other hand, can be decoupled for every wavenumber k_x and k_y, and for every chaos polynomial Γ_i, because no convolution is necessary, and the orthogonality of the chaos polynomials can be used. For example, the analog expression for

$A_\ell^{[1]}(\hat{\mathbf{U}}(k_x, k_y))$ in the deterministic part is simply given by

$$\left(\frac{2(1-\nu)}{1-2\nu}k_x^2\mathbf{\Phi} + k_y^2\mathbf{\Phi} - \bar{\mathbf{\Phi}}\right)\hat{\mathbf{U}}(k_x, k_y)\mathbf{D_\Gamma}, \tag{15}$$

which can be derived independently for every k_x and k_y.

The system of equations Eq. (11) can be transformed into a linear system by discretizing the horizontal wavenumber plane (k_x, k_y) and reordering, which leads to $(\mathbf{K_d} + \mathbf{K_s})\hat{\mathbf{x}} = \hat{\mathbf{b}}_{\text{ext}}$. The vector $\hat{\mathbf{x}}$ contains the unknown $\hat{u}_{ij}(\mathbf{k_x}, \mathbf{k_y}), \hat{v}_{ij}(\mathbf{k_x}, \mathbf{k_y})$ and $\hat{w}_{ij}(\mathbf{k_x}, \mathbf{k_y})$, $\hat{\mathbf{b}}_{\text{Ext}}$ is the reordered version of $\hat{\mathbf{F}}_{\text{Ext}}$. $\mathbf{K_d}$ contains the deterministic parts, and has a block tridiagonal structure. Unfortunately, $\mathbf{K_s}$ is densely populated and its size is given by the product of

- the number of FE ansatz functions $\phi_i(z)$,
- the expansion length of the KLE,
- the expansion length of the PCE,
- the number of grid points $\mathbf{k_x}$ and $\mathbf{k_y}$ used in the discretization of the system.

Even for small lengths of the stochastic expansions and a small number of discretization nodes $(\mathbf{k_x}, \mathbf{k_y})$, the stochastic matrix $\mathbf{K_s}$ gets very large, mainly because of the convolution of the eigenfunctions from the KLE and the unknown displacements. A direct solution of the system is no longer feasible.

Instead we propose an iteration procedure. As already mentioned, it is possible to decouple the deterministic part (and therefore $\mathbf{K_d}$) into subsystems with much smaller matrices which are only dependent on the number of FE layers and the type of the $\phi_i(z)$. A decomposition of these submatrices can be done efficiently with numerical schemes adapted to the block tridiagonal structure of the matrix (see for example Gansterer[23]).

The stochastic matrix $\mathbf{K_s}$ is drawn onto the right hand side and the system is solved using an iteration:

$$\begin{aligned}\mathbf{K_d}\hat{\mathbf{x}}_0 &= \hat{\mathbf{b}}_{\text{Ext}}\\ \mathbf{K_d}\hat{\mathbf{x}}_n &= \hat{\mathbf{b}}_{\text{Ext}} - \mathbf{K_s}\hat{\mathbf{x}}_{n-1} \text{ for } n > 0.\end{aligned} \tag{16}$$

There is no need to derive the matrix $\mathbf{K_s}$ explicitly, since only products of this matrix with a vector $\mathbf{x}$ are needed. To ensure the convergence of the iteration, it is sufficient that $\frac{G_s}{G_0} < 1$, which is the case in realistic scenarios. This can easily be seen by reformulating Eq. (16) into $\hat{\mathbf{x}}_n = \sum_{i=0}^{n}(-\mathbf{K_d}^{-1}\mathbf{K_s})^i\hat{\mathbf{x}}_\mathbf{0}$.

5. Implementational Details

It is clear that for a practical application, some modifications and simplifications have to be made. For the calculation of the eigenfunctions $f_\ell(x, y)$ of the Fredholm equation used in the KLE (Eq. (8)), a similar approach to the one in Ghanem and Spanos' book[6] is used. The integral of the Fredholm equation Eq. (9) is restricted to the finite interval

$[-\mathbf{a}, \mathbf{a}] = [-a_x, a_x] \times [-a_y, a_y]$. To numerically calculate the eigenfunctions and eigenvalues for arbitrary (bounded) covariance functions, the integral is approximated by quadrature, and Eq. (9) is transformed into a linear eigenvalue problem. To simplify calculations, it is assumed that the covariance function of the shear modulus $C(\mathbf{x_1}, \mathbf{x_2})$ is separable with respect to the spatial directions x and y, and therefore it can be written as $C(\mathbf{x_1}, \mathbf{x_2}) = C((x_1, y_1), (x_2, y_2)) = C_1(x_1, x_2)C_2(y_1, y_2)$. Using this assumption, it is possible to reformulate Eq. (8):

$$G(x, y, z, \theta) = G_0(z) + G_s \sum_{i,j} \sqrt{\lambda_i \mu_j} f_i(x) g_j(y) \xi_i(\theta) \xi_j(\theta)$$

and the eigenpairs (λ_i, f_i) and (μ_j, g_j) can be calculated independently. Additionally, $G(x, y, z, \theta)$ is assumed to be Gaussian; thus Hermite polynomials can be used in the PCE. The length of the KLE expansion is set to 4. Only the 2 biggest eigenpairs in each direction are considered.

For the discretization of the wavenumber domain (k_x, k_y), an equidistant grid $[\mathbf{k_x}]_i = -K_x + \frac{2K_x}{N_x} i,\ [\mathbf{k_y}]_j = -K_y + \frac{2K_y}{N_y} j\ (i = 0, \ldots, N_x,\ j = 0, \ldots, N_y)$ is used. To transform the calculated results from the Fourier domain back to the regular domain, a discrete Fourier transform is used. The transformation of the external load from the space-time domain into the wavenumber frequency domain is done analytically. After the Fourier transform with respect to x, y and t, the force $\hat{f}_{\text{Ext}}$ for a point load with strength P (see also Eq. (12)) is given by

$$\begin{aligned}
&\frac{P}{4a_x a_y} \int_{\infty}^{\infty} \int_{-a_x}^{a_x} \int_{-a_y}^{a_y} \delta(x - vt)\delta(y) \cos(2\pi\omega_0 t) e^{-2\pi \mathrm{i}(\frac{k_x x}{2a_x} + \frac{k_y y}{2a_y} + \omega t)} dy dx dt = \\
&\qquad \frac{P}{4a_x a_y} \int_{\infty}^{\infty} \int_{-a_x}^{a_x} \delta(x - vt) \cos(2\pi\omega_0 t) e^{-2\pi \mathrm{i}(\frac{k_x x}{2a_x} + \omega t)} dx dt = \\
&\qquad\qquad \frac{P}{4a_x a_y} \int_{\infty}^{\infty} e^{-2\pi \mathrm{i} \frac{k_x v}{2a_x}} \cos(2\pi\omega_0 t) e^{-2\pi \mathrm{i}\omega t} dt = \\
&\qquad\qquad \frac{P}{8a_x a_y} \left(\delta(\omega + \frac{k_x v}{2a_x} + \omega_0) + \delta(\omega + \frac{k_x v}{2a_x} - \omega_0) \right). \qquad (17)
\end{aligned}$$

For practical purposes it is assumed in Eq. (17), that the solution is periodic in the spatial domain $[-a_x, a_x] \times [-a_y, a_y]$. This can be motivated by the fact that we have to restrict the wavenumber domain (k_x, k_y) to a finite interval $[-K_x, K_x] \times [-K_y, K_y]$, and the numerical Fourier back transformation from this domain to the regular spatial domain therefore results in a periodic function. For the Fourier transformation with respect to the time t, such an assumption was not used. Please note, that the standard problem of assuming compact support in space, time and frequency exists here. While this is not possible in an exact sense, it is possible to achieve this in an approximate sense[24,25]. In the discrete version,

pulses take the role of the delta functional, which means that the right hand side is only non-zero for certain frequencies ω_i that satisfy $\omega_i = -\frac{v\cdot[\mathbf{k_x}]_i}{2a_x} \pm \omega_0$ $(i = 0, \ldots, N_x)$.

In the same way, the right hand side for the box load Eq. (13) can be derived:

$$\frac{P}{8a_x a_y}\mathrm{sinc}\left(\frac{\pi b_1 k_x}{2a_x}\right)\mathrm{sinc}\left(\frac{\pi b_2 k_y}{2a_y}\right)\left(\delta(\omega + \frac{k_x v}{2a_x} - \omega_0) + \delta(\omega + \frac{k_x v}{2a_x} + \omega_0)\right). \qquad (18)$$

Because of the space-time coupling by the movement, the discretization of the wavenumber domain k_x automatically defines a frequency grid. For each grid point with respect to k_x there are only two possible frequencies where the right hand side of the global system is not zero. This coupling should be taken into account when choosing the spatial range in the x-direction. Roughly spoken, the size of the spatial domain should be consistent with the frequency of the moving load and its velocity. The easiest way is to choose the size of the spatial domain in a way that ensures that the load can be continued periodically over this domain. In the following example it is assumed that x is between -30 and 30, which matches a moving load oscillating with a frequency of 30 Hz, moving with a velocity of 60 m/s along the x-axis. We also use the same spatial grid for the discretization and the numerical solution of the Fredholm equation.

6. Example

In this example, the soil is modelled using 2 stochastic layers and a final half space. The stochastic layers were subdivided into FE-layers with a width of 0.1 m each. For each layer, the shear modulus G_0 is assumed to be constant over all sublayers, for the first layer, we chose $G_0 = 3.74{\cdot}10^7 + 3.74{\cdot}10^6\mathrm{i}$ N/m^2, where $\mathrm{i}^2 = -1$. The variance scaling factor G_s was set to $G_s = 3.74{\cdot}10^6 + 3.74{\cdot}10^5\mathrm{i}$, the layers has a Poisson ratio of $\nu = 0.3333333$ and a density of $\rho = 1500$ kg/m^3. For the parameters of the other layers, please refer to Table 1. As covariance function an exponential functions $C(\mathbf{x}_1, \mathbf{x}_2) = e^{-5|\mathbf{x}_1 - \mathbf{x}_2|}$ was used (see also Ghanem and Spanos[6]). All material parameters were derived from a seismic measurement,

	Layer 1	Layer 2	Half space
G	$3.74 \cdot 10^7 + 3.74 \cdot 10^6\mathrm{i}$	$1.183 \cdot 10^8 + 1.183 \cdot 10^7\mathrm{i}$	$1.35 \cdot 10^8 + 6.75 \cdot 10^6\mathrm{i}$
G_0	$3.74 \cdot 10^6 + 3.74 \cdot 10^5\mathrm{i}$	$1.35 \cdot 10^7 + 6.75 \cdot 10^5\mathrm{i}$	
ν	0.33333	0.3147	0.3147
ρ	1500	1750	2000
d	2	6	

Table 1. Material parameter for the soil model.

the first layer represents some aggradation, the second layer consist of dry sand and slit. To test our choice of material parameters, the relative velocity levels at 30 m and 50 m with respect to 10 m distance from the vibration (point) source are compared in Fig. 1.

The calculated and the measured data agree good enough, which indicates a good choice of material parameters.

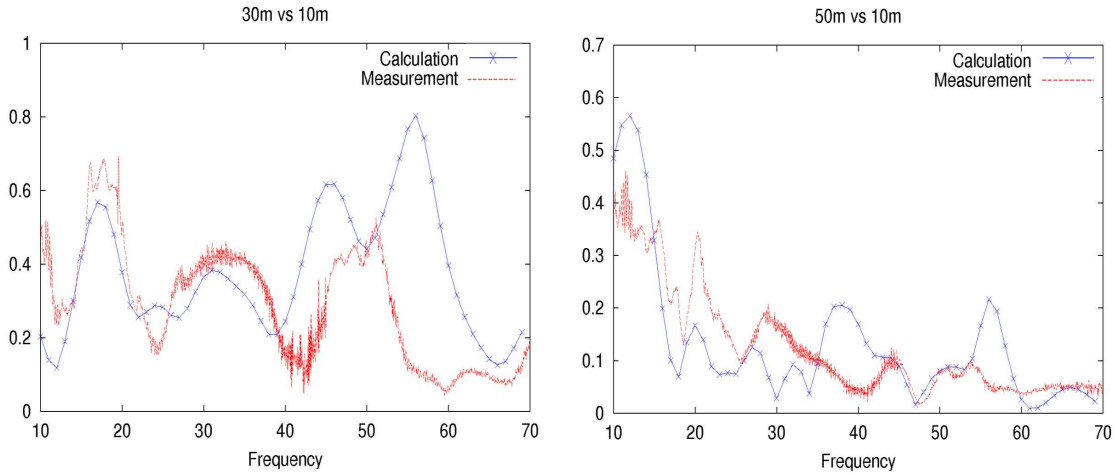

Fig. 1. Relative velocity level at 30 m and 50 m with respect to 10 m distance from the source

As ansatz functions $\boldsymbol{\phi}(z)$ in Eq. (6), second order B-splines are used:

$$\phi_0(z) = \begin{cases} 0 & z < z_0 \\ \frac{z_1 - z}{z_1} & z_0 \le z < z_1, \\ 0 & z \ge z_1 \end{cases} \qquad \phi_j(z) = \begin{cases} 0 & 0 \le z < z_{j-1} \\ \frac{z - z_{j-1}}{z_j - z_{j-1}} & z_{j-1} \le z < z_j \\ \frac{z_{j+1} - z}{z_{j+1} - z_j} & z_j \le z \le z_{j+1} \\ 0 & z \ge z_{j+1} \end{cases}.$$

For the PCE, we only use polynomials with maximum order 2, thus, together with the length of the KLE, we get $N+1 = \frac{(4+2)!}{4!2!} = 15$ different Hermite polynomials. For the spatial grid in the wavenumber domain we choose $61 \cdot 61$ equidistant grid points in the interval $[-\pi, \pi] \times [-\pi, \pi]$. As a load we assume a point load which oscillates with a frequency of 30 Hz (trains have frequency components between 10 Hz and 60 Hz) and moves along the x-axis with a speed of 60 m/s. Like in the work of Celebi and Schmid[26] the amplitude of the moving force is assumed to be 1kN.

With these assumptions, the deterministic matrix $\mathbf{K_d}$ consists of $15{\cdot}61{\cdot}61$ diagonal blocks (one for each chaos polynomial and each grid point of the discretization of the wavenumber domain), and each of these subsystems consists of 6×6 big diagonal blocks (one for each FE layer). Blocks of adjacent layers have a 3×3 overlap (the displacement on top of one layer equals the displacement at the bottom of the previous layer). Because of the orthogonality of the Hermite polynomials and our choice of FE ansatz functions, the mean value for the z-displacements on top is simply given by $\mathbb{E}(w(x, y, 0, \theta)) = \sum_{j=0}^{N} w_{0j}(x, y)\phi_0(0)\mathbb{E}(\Gamma_j) = w_{00}(x, y)$. The variance can be calculated by $\sum_{j=1}^{N} w_{0j}^2 \mathbb{E}(\Gamma_j^2)$ (see also Eq. (10)).

Fig. 2 shows the mean value of the z-component of the displacements and their standard

deviation on top of the soil (top row) and the same data at a depth of 2 m (bottom row) at different time steps. The maximum of the displacements in the z-direction in a distance of 2 m from the source on top of the soil is about 1.5 μm, which is in the same range as the results found in the paper of Celebi and Schmid[26], who investigated ground vibrations with the help of BEM and thin layer methods. In this example, we used a relatively small G_s to reduce the number of iterations, thus the standard deviation of the displacements is relatively small. The periodicity in the each of the subfigure is because of the Fourier transformation and our assumption of a periodic force. Still, the size of the grid (60 m $\times$ 60 m) was chosen big enough not to produce too much interference between the waves (some smaller interferences can be found for the standard deviation in a distance of 40 m from the source). It can be observed that in a depth of 2 m the fine structure of the wave propagation is reduced compared to the top.

To demonstrate the convergence of the iteration, calculations with different values for the stochastic scaling factor G_s were made. In Fig. 3, the logarithm of the residuum $r = ||\mathbf{K}\hat{\mathbf{x}} - \hat{\mathbf{b}}_{\text{Ext}}||$ after each iteration step for different values of the factor $\frac{G_s}{G_0}$ is shown. As expected, an exponential convergence rate can be observed.

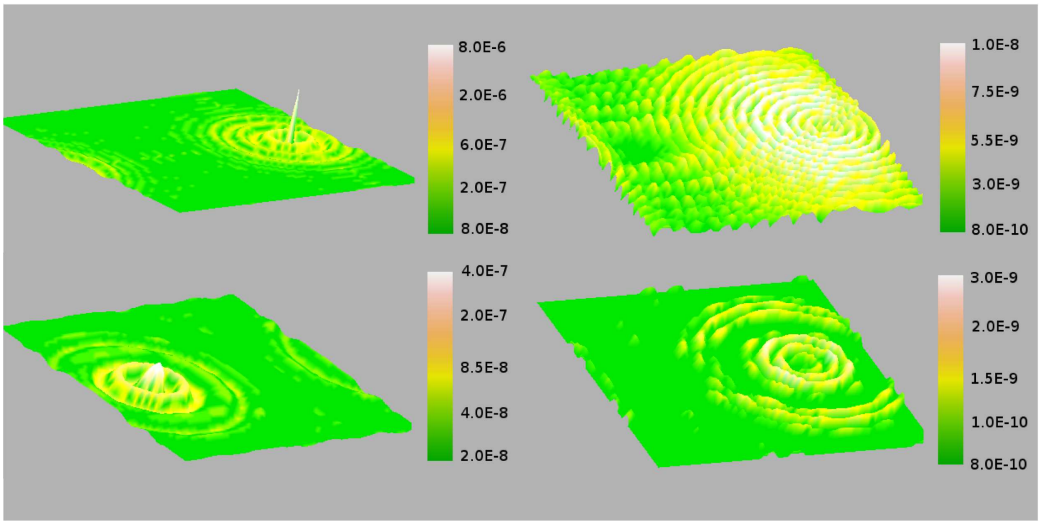

Fig. 2. Mean value and standard deviation of the displacement in the z direction for different time steps and different depths. Top: mean value and standard deviation for the displacement on top of the layers at time step 10. Bottom left: mean value (timestep 4) and standard deviation (time step 10) of the displacement at a depth of 2 m. The units on the colorbar are in meters.

7. Conclusion and Outlook

A 3D-model to numerically calculate the propagation of waves in layers with stochastic material parameters was presented. Based on the Karhunen Loeve expansion and the Chaos

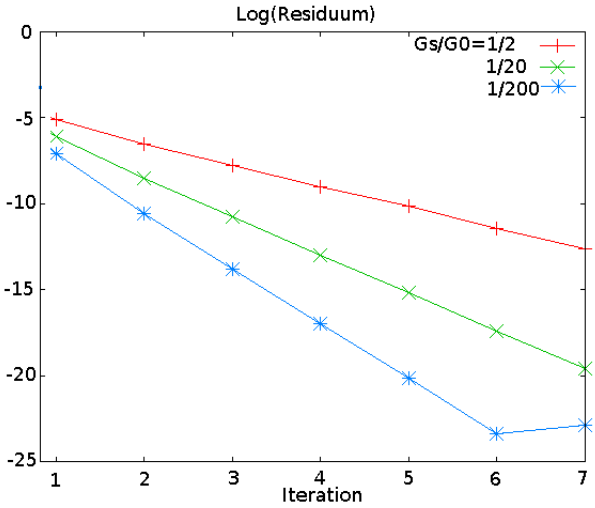

Fig. 3. Error after each iteration for three different values of G_s/G_0.

polynomial expansion, it is possible to decouple the system in the wavenumber-frequency domain into a stochastic part, which is fully coupled for all wavenumbers and all chaos polynomials, and a deterministic part, which can be represented by a sparse block-tridiagonal matrix. The linear system describing the system is solved with an iteration, where only the sparse deterministic matrix has to be inverted.

Future work will mainly be focused on enhancing the efficiency of the program code. One question will be the choice of a suitable grid in the wavenumber domain. From numerical experience, we know that in the wavenumber-frequency domain the solution of the system with non-moving load with low frequency varies mostly inside a small area around the center where the load is placed. Thus a fine (k_x, k_y) grid should be used there. Outside the interval the solution is very smooth and, compared to the values around the origin, small. Therefore a much coarser grid can be used in that area to reduce computation time. Also the topic of parallelization will play an important role. When applying moving loads, results for different frequencies have to be calculated, which can be done independently, thus providing a good possibility to parallelize calculations.

ACKNOWLEDGEMENTS. The authors would like to thank Piotr Majdak and Johnny White for useful comments, suggestions and proofreading. This work was partially funded by the Austrian Science Fund FWF: Pr. P-16224-NO7.

Appendix

A. Matrixparts

In Section 4, the linear system of equations that describes our model is given by:

$$G_0\mathbf{A}_d^{[1]}(\hat{\mathbf{U}},\hat{\mathbf{V}},\hat{\mathbf{W}})+G_s\sum_\ell\left(\mathbf{A}_\ell^{[1]}(\hat{\mathbf{U}})+\mathbf{A}_\ell^{[2]}(\hat{\mathbf{V}})+\mathbf{A}_\ell^{[3]}(\hat{\mathbf{W}})\right)-\rho\omega^2\mathbf{\Phi}\hat{\mathbf{U}}\mathbf{D}_\Gamma=\mathbf{0}$$
$$G_0\mathbf{A}_d^{[2]}(\hat{\mathbf{U}},\hat{\mathbf{V}},\hat{\mathbf{W}})+G_s\sum_\ell\left(\mathbf{A}_\ell^{[4]}(\hat{\mathbf{U}})+\mathbf{A}_\ell^{[5]}(\hat{\mathbf{V}})+\mathbf{A}_\ell^{[6]}(\hat{\mathbf{W}})\right)-\rho\omega^2\mathbf{\Phi}\hat{\mathbf{V}}\mathbf{D}_\Gamma=\mathbf{0}$$
$$G_0\mathbf{A}_d^{[3]}(\hat{\mathbf{U}},\hat{\mathbf{V}},\hat{\mathbf{W}})+G_s\sum_\ell\left(\mathbf{A}_\ell^{[7]}(\hat{\mathbf{U}})+\mathbf{A}_\ell^{[8]}(\hat{\mathbf{V}})+\mathbf{A}_\ell^{[9]}(\hat{\mathbf{W}})\right)-\rho\omega^2\mathbf{\Phi}\hat{\mathbf{W}}\mathbf{D}_\Gamma=\hat{\mathbf{F}}_{\mathrm{Ext}}.$$

The entries of the "stochastic" matrices $\left[A_\ell^{[*]}\right]_{ij}$ are given by (i and j denote the number of the row and the column respectively). All definitions are the same as in Sections 2 and 4:

$$\begin{aligned}\left[\mathbf{A}_\ell^{[1]}(\hat{\mathbf{U}}(k_x,k_y))\right]_{ij}=&\\ &\frac{2(1-\nu)}{1-2\nu}\int_{-\infty}^{\infty}\int_{-\infty}^{\infty}k_xk_x'\hat{f}_\ell(k_x-k_x',k_y-k_y')\left[\mathbf{\Phi}\hat{\mathbf{U}}(k_x',k_y')\mathbf{\Gamma}_\ell\right]_{ij}dk_x'dk_y'+\\ &+\int_{-\infty}^{\infty}\int_{-\infty}^{\infty}k_yk_y'\hat{f}_\ell(k_x-k_x',k_y-k_y')\left[\mathbf{\Phi}\hat{\mathbf{U}}(k_x',k_y')\mathbf{\Gamma}_\ell\right]_{ij}dk_x'dk_y'-\\ &-\int_{-\infty}^{\infty}\int_{-\infty}^{\infty}\hat{f}_\ell(k_x-k_x',k_y-k_y')\left[\bar{\mathbf{\Phi}}\hat{\mathbf{U}}(k_x',k_y')\mathbf{\Gamma}_\ell\right]_{ij}dk_x'dk_y'.\end{aligned}$$

$$\begin{aligned}\left[\mathbf{A}_\ell^{[2]}(\hat{\mathbf{V}}(k_x,k_y))\right]_{ij}=&\\ &\frac{2\nu}{1-2\nu}\int_{-\infty}^{\infty}\int_{-\infty}^{\infty}k_xk_y'\hat{f}_\ell(k_x-k_x',k_y-k_y')\left[\mathbf{\Phi}\hat{\mathbf{V}}(k_x',k_y')\mathbf{\Gamma}_\ell\right]_{ij}dk_x'dk_y'+\\ &+\int_{-\infty}^{\infty}\int_{-\infty}^{\infty}k_yk_x'\hat{f}_\ell(k_x-k_x',k_y-k_y')\left[\mathbf{\Phi}\hat{\mathbf{V}}(k_x',k_y')\mathbf{\Gamma}_\ell\right]_{ij}dk_x'dk_y'\end{aligned}$$

$$\Big[\mathbf{A}_\ell^{[3]}(\hat{\mathbf{W}}(k_x,k_y))\Big]_{ij} =$$
$$\mathrm{i}\frac{2\nu}{1-2\nu}\int\limits_{-\infty}^{\infty}\int\limits_{-\infty}^{\infty} k_x\hat{f}_\ell(k_x-k'_x,k_y-k'_y)\left[\boldsymbol{\Phi}'^{\mathbf{T}}\hat{\mathbf{W}}(k'_x,k'_y)\boldsymbol{\Gamma}_\ell\right]_{ij}dk'_xdk'_y+$$
$$+\,\mathrm{i}\int\limits_{-\infty}^{\infty}\int\limits_{-\infty}^{\infty} k'_x\hat{f}_\ell(k_x-k'_x,k_y-k'_y)\left[\boldsymbol{\Phi}'\hat{\mathbf{W}}(k'_x,k'_y)\boldsymbol{\Gamma}_\ell\right]_{ij}dk'_xdk'_y$$

$$\Big[\mathbf{A}_\ell^{[4]}(\hat{\mathbf{U}}(k_x,k_y))\Big]_{ij} =$$
$$\frac{2\nu}{1-2\nu}\int\limits_{-\infty}^{\infty}\int\limits_{-\infty}^{\infty} k_yk'_x\hat{f}_\ell(k_x-k'_x,k_y-k'_y)\left[\boldsymbol{\Phi}\hat{\mathbf{U}}(k'_x,k'_y)\boldsymbol{\Gamma}_\ell\right]_{ij}dk'_xdk'_y+$$
$$+\int\limits_{-\infty}^{\infty}\int\limits_{-\infty}^{\infty} k_xk'_y\hat{f}_\ell(k_x-k'_x,k_y-k'_y)\left[\boldsymbol{\Phi}\hat{\mathbf{U}}(k'_x,k'_y)\boldsymbol{\Gamma}_\ell\right]_{ij}dk'_xdk'_y$$

$$\Big[\mathbf{A}_\ell^{[5]}(\hat{\mathbf{V}}(k_x,k_y))\Big]_{ij} =$$
$$\frac{2(1-\nu)}{1-2\nu}\int\limits_{-\infty}^{\infty}\int\limits_{-\infty}^{\infty} k_yk'_y\hat{f}_\ell(k_x-k'_x,k_y-k'_y)\left[\boldsymbol{\Phi}\hat{\mathbf{V}}(k'_x,k'_y)\boldsymbol{\Gamma}_\ell\right]_{ij}dk'_xdk'_y+$$
$$+\int\limits_{-\infty}^{\infty}\int\limits_{-\infty}^{\infty} k_xk'_x\hat{f}_\ell(k_x-k'_x,k_y-k'_y)\left[\boldsymbol{\Phi}\hat{\mathbf{V}}(k'_x,k'_y)\boldsymbol{\Gamma}_\ell\right]_{ij}dk'_xdk'_y-$$
$$-\int\limits_{-\infty}^{\infty}\int\limits_{-\infty}^{\infty} \hat{f}_\ell(k_x-k'_x,k_y-k'_y)\left[\bar{\boldsymbol{\Phi}}\hat{\mathbf{V}}(k'_x,k'_y)\boldsymbol{\Gamma}_\ell\right]_{ij}dk'_xdk'_y$$

$$\Big[\mathbf{A}_\ell^{[6]}(\hat{\mathbf{W}}(k_x,k_y))\Big]_{ij} =$$
$$\mathrm{i}\frac{2\nu}{1-2\nu}\int\limits_{-\infty}^{\infty}\int\limits_{-\infty}^{\infty} k_y\hat{f}_\ell(k_x-k'_x,k_y-k'_y)\left[\boldsymbol{\Phi}'^{\mathbf{T}}\hat{\mathbf{W}}(k'_x,k'_y)\boldsymbol{\Gamma}_\ell\right]_{ij}dk'_xdk'_y+$$
$$\mathrm{i}\int\limits_{-\infty}^{\infty}\int\limits_{-\infty}^{\infty} k'_y\hat{f}_\ell(k_x-k'_x,k_y-k'_y)\left[\boldsymbol{\Phi}'\hat{\mathbf{W}}(\mathbf{k'_x},\mathbf{k'_y})\boldsymbol{\Gamma}_\ell\right]_{ij}dk'_xdk'_y$$

$$\left[\mathbf{A}_\ell^{[7]}(\hat{\mathbf{U}}(k_x,k_y)\right]_{ij} =$$
$$\mathrm{i}\frac{2\nu}{1-2\nu}\int_{-\infty}^{\infty}\int_{-\infty}^{\infty} k'_x\hat{f}_\ell(k_x-k'_x,k_y-k'_y)\left[\mathbf{\Phi'}\hat{\mathbf{U}}(\mathbf{k'_x},\mathbf{k'_y})\mathbf{\Gamma}_\ell\right]_{ij}dk'_xdk'_y+$$
$$+\mathrm{i}\int_{-\infty}^{\infty}\int_{-\infty}^{\infty} k_x\hat{f}_\ell(k_x-k'_x,k_y-k'_y)\left[\mathbf{\Phi'^T}\hat{\mathbf{U}}(k'_x,k'_y)\mathbf{\Gamma}_\ell\right]_{ij}dk'_xdk'_y$$

$$\left[\mathbf{A}_\ell^{[8]}(\hat{\mathbf{V}}(k_x,k_y))\right]_{ij} =$$
$$\mathrm{i}\frac{2\nu}{1-2\nu}\int_{-\infty}^{\infty}\int_{-\infty}^{\infty} k'_y\hat{f}_\ell(k_x-k'_x,k_y-k'_y)\left[\mathbf{\Phi'}\hat{\mathbf{V}}(k'_x,k'_y)\mathbf{\Gamma}_\ell\right]_{ij}dk'_xdk'_y+$$
$$+\mathrm{i}\int_{-\infty}^{\infty}\int_{-\infty}^{\infty} k_y\hat{f}_\ell(k_x-k'_x,k_y-k'_y)\left[\mathbf{\Phi'^T}\hat{\mathbf{V}}(k'_x,k'_y)\mathbf{\Gamma}_\ell\right]_{ij}(k'_x,k'_y)dk'_xdk'_y$$

$$\left[\mathbf{A}_\ell^{[9]}(\hat{\mathbf{W}}(k_x,k_y))\right]_{ij} =$$
$$-\frac{2(1-\nu)}{1-2\nu}\int_{-\infty}^{\infty}\int_{-\infty}^{\infty}\hat{f}_\ell(k_x-k'_x,k_y-k'_y)\left[\bar{\mathbf{\Phi}}\hat{\mathbf{W}}(k'_x,k'_y)\mathbf{\Gamma}_\ell\right]_{ij}dk'_xdk'_y+$$
$$+\int_{-\infty}^{\infty}\int_{-\infty}^{\infty} k_xk'_x\hat{f}_\ell(k_x-k'_x,k_y-k'_y)\left[\mathbf{\Phi}\hat{\mathbf{W}}(k'_x,k'_y)\mathbf{\Gamma}_\ell\right]_{ij}dk'_xdk'_y+$$
$$+\int_{-\infty}^{\infty}\int_{-\infty}^{\infty} k_yk'_y\hat{f}_\ell(k_x-k'_x,k_y-k'_y)\left[\mathbf{\Phi}\hat{\mathbf{W}}(k'_x,k'_y)\mathbf{\Gamma}_\ell\right]_{ij}dk'_xdk'_y$$

The "deterministic" part is defined by

$$\begin{aligned}
\mathbf{A}_d^{[1]}(\hat{\mathbf{U}},\hat{\mathbf{V}},\hat{\mathbf{W}}) &= \left(\frac{2(1-\nu)}{1-2\nu}k_x^2\boldsymbol{\Phi}+k_y^2\boldsymbol{\Phi}+\bar{\boldsymbol{\Phi}}\right)\hat{\mathbf{U}}(k_x,k_y)\mathbf{D}_\Gamma+\\
&\quad+k_xk_y\boldsymbol{\Phi}\frac{1}{1-2\nu}\hat{\mathbf{V}}(k_x,k_y)\mathbf{D}_\Gamma+\mathrm{i}k_x\left(\frac{2\nu}{1-2\nu}\boldsymbol{\Phi}'^T+\boldsymbol{\Phi}'\right)\hat{\mathbf{W}}(k_x,k_y)\mathbf{D}_\Gamma\\
\mathbf{A}_d^{[2]}(\hat{\mathbf{U}},\hat{\mathbf{V}},\hat{\mathbf{W}}) &= \left(\frac{2(1-\nu)}{1-2\nu}k_y^2\boldsymbol{\Phi}+k_x^2\boldsymbol{\Phi}+\bar{\boldsymbol{\Phi}}\right)\hat{\mathbf{V}}(k_x,k_y)\mathbf{D}_\Gamma+\\
&\quad+k_xk_y\boldsymbol{\Phi}\frac{1}{1-2\nu}\hat{\mathbf{U}}(k_x,k_y)\mathbf{D}_\Gamma+\mathrm{i}k_y\left(\frac{2\nu}{1-2\nu}\boldsymbol{\Phi}'^T+\boldsymbol{\Phi}'\right)\hat{\mathbf{W}}(k_x,k_y)\mathbf{D}_\Gamma\\
\mathbf{A}_d^{[3]}(\hat{\mathbf{U}},\hat{\mathbf{V}},\hat{\mathbf{W}}) &= \left(\boldsymbol{\Phi}(k_x^2+k_y^2)+\frac{2(1-\nu)}{1-2\nu}\bar{\boldsymbol{\Phi}}\right)\hat{\mathbf{W}}(k_x,k_y)\mathbf{D}_\Gamma+\\
&\quad+\mathrm{i}\left(\boldsymbol{\Phi}'^T+\frac{2\nu}{1-2\nu}\boldsymbol{\Phi}'\right)\left(\hat{\mathbf{U}}(k_x,k_y)+\hat{\mathbf{V}}(k_x,k_y)\right)\mathbf{D}_\Gamma.
\end{aligned}$$

References

1. H. Antes, P. Borejko, and F. Ziegler. Seismic waves in an impacted half-space: Time domain BEM versus the method of generalized ray. In C. A. Brebbia and G. S. Gipson, editors, *Boundary Elements XIII*, pages 457–470. Elsevier Science, London, 1991.
2. A. K. Belyaev and F. Ziegler. Uniaxial waves in randomly heterogeneous elastic media. *Int. Journal of Probabilistic Engineering Mechanics*, 13(1):27–38, 1998.
3. P. Borejko and F. Ziegler. Seismic waves in layered soil: The generalized ray theory. In *Structural Dynamics - Recent Advances*, pages 52–90. Springer, Berlin, 1991.
4. L. Lehmann. An effective finite element approach for soil-structure analysis in the time-domain. *Struct. Engng. Mech.*, 21(4):437–450, 2005.
5. G. D. Manolis. Stochastic soil dynamics. *Soil Dynamics and Earthquake Engineering*, 22:3–15, 2002.
6. R. G. Ghanem and P. D. Spanos. *Stochastic Finite Elements: A Spectral Approach*. Springer-Verlag, New York Berlin Heidelberg London Paris Tokyo Hong Kong Barcelona, 1991.
7. D. Xiu. Fast numerical methods for stochastic computations: A review. *Commun. Comput. Phys.*, 5(2-4):242–272, 2009.
8. P. Balazs, W. Kreuzer, and H. Waubke. A stochastic 2D-model for calculating vibrations in random layers. *Journal of Computational Acoustics*, 15(3):271–283, 2007.
9. H. Waubke. *Dynamische Berechnungen für den Halbraum mit streuenden Parametern mittels orthogonaler Polynome*. PhD thesis, Technische Universität München, 1996. Berichte aus dem Konstruktiven Ingenieurbau.
10. R. G. Ghanem and R. M. Kruger. Numerical solution of spectral stochastic finite element systems. *Comput. Methods Appl. Mech. Engng.*, 129:289–303, 1996.
11. S.P. Huang, S.T. Quek, and K.K. Phoon. Convergence study of the truncated Karhunen-Loeve expansion for simulation of stochastic processes. *Int. J. Numer. Meth. Engng*, 52:1029–1043, 2001.
12. K.K. Phoon, H.W. Huang, and S.T. Quek. Comparison between Karhunen-Loeve and wavelet expansions for simulation of Gaussian processes. *Comput. Struct.*, 82:985–991, 2004.
13. J. E. Castrillón-Candás and K Amaratunga. Fast estimation of continuous Karhunen-Loeve eigenfunctions using wavelets. *IEEE T Signal Proces.*, 50(1), 2002.

14. B. J. Debusschere, H. N. Najm, P. P. Pébay, O. M. Knio, R. G. Ghanem, and O. P. Le Maitre. Numerical challenges in the use of polynomial chaos representations for stochastic processes. *SIAM J. Sci. Comp.*, 26(2):698–719, 2004.
15. X. Wan and G. E. Karniadakis. Multi-element generalized polynomial chaos for arbitrary probability measures. *SIAM J. Sci. Comput.*, 28:901–928, 2006.
16. Dongbin Xiu and George EM Karniadakis. The Wiener-Askey polynomial chaos for stochastic differential equations. *SIAM J. Sci. Comput.*, 24(2):619–644, 2002.
17. N. Wiener. The homogeneous chaos. *Am. J. Math.*, 60:897–936, 1938. John Hopkins Press, Baltimore.
18. M. Berveiller, B. Sudret, and M. Lemaire. Stochastic finite element: a non intrusive approach by regression. *Revue Européene de Mécanique Numérique*, 15:81–92, 2006.
19. L. Auersch. The effect of critically moving loads on the vibrations of soft soils and isolated railway tracks. *J. Sound Vib.*, 310:587–607, 2007.
20. A. V. Pesterev, L. A. Bergman, C. A. Tan, T.-C. Tsao, and B. Yang. Some recent results in moving load problems with application to highwys bridges. *Proc. Int. Conf. Motion Vib. Control*, 6(1):K.20–K.27, 2002.
21. H. Takemiya. Simulation of track-ground vibrations due to a high-speed train: the case of X-2000 at Ledsgard. *J. Sound Vib.*, 261:503–526, 2003.
22. Y. L. Xu and X. J. Hong. Stochastic modelling of traffic-induced building vibration. *J. Sound Vib.*, 313:149–170, 2008.
23. Wilfried N. Gansterer. Computing orthogonal decompositions of block tridiagonal or banded matrices. In *International Conference on Computational Science (1)*, Lecture Notes in Computer Science, pages 25–32. Springer-Verlag, Berlin, Heidelberg, New York, Tokyo, May 2005.
24. Norbert Kaiblinger. Approximation of the Fourier transform and the dual Gabor window. *J. Fourier Anal. Appl.*, 11(1):25–42, 2005.
25. Peter L. Søndergaard. Gabor frames by sampling and periodization. *Adv. Comput. Math.*, 27(4):355–373, 2007.
26. E. Celebi and G. Schmid. Investigation of ground vibrations induced by moving loads. *Eng. Struct.*, 27:1981–1998, 2005.